Morphology Control and Transferability of Ordered Through-Pore Arrays Based on the Electrodeposition of a Colloidal Monolayer

ARTICLE *in* ADVANCED MATERIALS · JULY 2004

Impact Factor: 17.49 · DOI: 10.1002/adma.200400006

7 AUTHORS, INCLUDING:

Fengqiang Sun
South China Normal University
56 PUBLICATIONS **1,569** CITATIONS
SEE PROFILE

Bingqiang Cao
University of Jinan (Jinan, China)
115 PUBLICATIONS **3,012** CITATIONS
SEE PROFILE

Fang Lu
Brookhaven National Laboratory
22 PUBLICATIONS **777** CITATIONS
SEE PROFILE

Guotao Duan
Chinese Academy of Sciences
83 PUBLICATIONS **2,638** CITATIONS
SEE PROFILE

ADVANCED MATERIALS

Morphology Control and Transferability of Ordered Through-Pore Arrays Based on Electrodeposition and Colloidal Monolayers**

By *Fengqiang Sun*, *Weiping Cai*,* *Yue Li*, *Bingqiang Cao*, *Fang Lu*, *Guotao Duan*, and *Lide Zhang*

Ordered porous films have received considerable attention in recent years[1–5] due to their unique properties and potential applications in catalysis,[1] photonic crystals,[2] optoelectronic devices,[3] etc. They are also excellent substrates for surface-enhanced Raman spectroscopy (SERS)[5] and cell cultures.[6] There are many techniques available for the formation of porous films, such as electron-beam lithography,[7] micro-contact printing,[8] electrochemical etching,[9] self-assembly,[10,11] and particle-array template methods,[12] some of which can be used to control the morphology of the films to a certain degree, which is obviously important for the applications and the properties of the films. A recently reported technique—the colloidal-crystal template approach—is very promising for the fabrication of ordered porous materials with controlled morphologies, as has been shown by the synthesis of three-dimensional (3D) photonic crystals[13] and some surface nanostructures.[14] The templates used in this method are mainly 3D colloidal crystals. Two-dimensional (2D) colloidal crystals, especially colloidal monolayers, have generally been used as masks for the fabrication of periodical particle arrays, which have been studied extensively.[15–17] In addition, they could also be excellent templates for the synthesis of ordered pore arrays (films) with one-pore thickness.[18] Several groups have synthesized TiO_2 and poly(divinylbenzene) porous films by combining the spray-pyrolysis technique[1] and the sol–gel technique, respectively,[6] and a selective dissolution procedure.[19] However, the challenge of producing ordered porous films with controlled morphologies and one-pore thickness still remains. To obtain such structures, it is necessary that the film grows from the bottom. As is well known, electrodeposition is an effective method to make a material grow from the bottom and has been used to synthesize 3D ordered porous materials based on 3D colloidal crystal templates.[20–22] Recently, noble metal (Au, Ag, and Pt) ordered porous films have also been reported using a colloidal monolayer as a template.[23] The pores possess a bowl-like shape and the diameters of the openings at the film surface can be tuned by the electrodeposition time to some degree. In this communication we introduce a strategy—heated template-directed electrodeposition—for the synthesis of morphology-controlled ordered through-pore arrays with one pore thickness. The film morphology can be controlled by heating the colloidal-monolayer-coated substrate, and electrodeposition. We have synthesized a series of metal, oxide, and semiconductor through-pore arrays with controlled morphologies. More interestingly, the deposited film can be transferred onto any desired substrate, especially onto an insulating substrate or curved surface, neither of which can normally be used for electrodeposition. As far as we know there are no other methods to transfer a pure film to another surface easily.

We chose gold as a good example to demonstrate the morphology-controlled fabrication of 2D ordered pore-arrays based on electrodeposition and a colloidal monolayer because, as a noble metal, it has found many applications in areas such as catalysis,[24] sensors,[25] molecular electronics,[26] and optics[27] (all associated with different morphologies).

Scheme 1 shows our fabrication procedure. First, a large-area (more than 1 cm^2) colloidal monolayer composed of polystyrene spheres (PSs) was synthesized on a glass substrate by spin-coating.[28] We then transferred this monolayer onto a conducting substrate (indium tin oxide (ITO)-coated glass) by a floating-transfer method.[16,18] After being dried in air at room temperature, the substrate coated with the monolayer was heated in an oven to 110 °C, which is higher than the glass-transition point of the PSs,[29–31] for a given time to bond the monolayer to the substrate. Such heating induces an area contact, instead of a point contact, between the PSs and the substrate, depending on the time, and this enlarged area contact increases the binding force (van der Waals' force[32]) between the PSs and the substrate. Finally, this substrate was used as the working electrode in a three-electrode electrolytic cell, with a graphite plate as the auxiliary electrode, a saturated calomel electrode (SCE) as the reference electrode, and an aqueous $HAuCl_4$ solution as the electrolyte. After electrodeposition at a constant electric potential for a certain time, an ordered through-pore array was formed by dissolving the monolayer in methylene chloride (CH_2Cl_2). Obviously, the morphology of the film can be controlled by heating the monolayer-coated substrate and subsequent electrodeposition. The bottom and top diameters of the through-pores, and the pore shapes, depend on the heating time; the film thickness is controlled by the deposition time. Based on the pore sizes at the bottom and the surface of the film, it is easy to roughly determine the film thickness without having to consider the curvature change of the PSs during the heating stage before deposition.

Figure 1 shows the through-pore arrays after substrate-heating and subsequent electrodeposition for different periods of time. All samples were electrodeposited at a potential of 0.7 V vs. SCE. Upon increasing the heating time of the

[*] Prof. W. P. Cai, F. Sun, Y. Li, B. Cao, F. Lu, G. Duan, Prof. L. Zhang
Key Laboratory of Materials Physics
Institute of Solid State Physics, Chinese Academy of Sciences
Hefei, 230031 (P.R. China)
E-mail: wpcai@issp.ac.cn

[**] This work was supported by the National Natural Science Foundation of China (grant number: 50271069), and the Royal Society (China–UK Joint Project No. 15280).

  DOI: 10.1002/adma.200400006

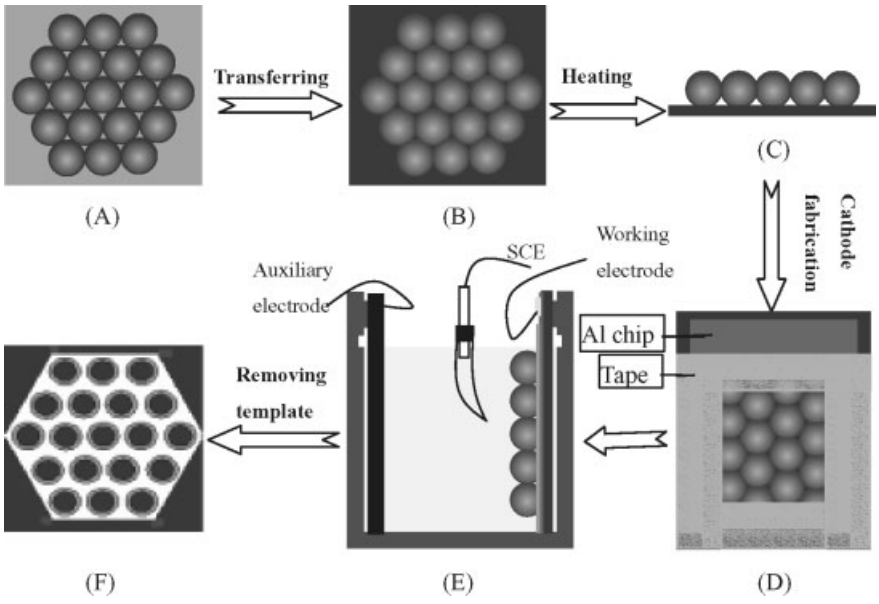

Scheme 1. Outline of the electrodeposition approach based on a colloidal monolayer crystal. A) Polystyrene colloidal monolayer on a glass substrate. B) The monolayer on the conductive substrate (ITO glass). C) The monolayer is bonded to the ITO glass by heating. D) Design of the cathode. E) Electrodeposition in a custom-built cell. F) Ordered through-pore array after removal of the monolayer.

monolayer-coated substrate before deposition (the PSs are 1000 nm in diameter), the openings at the film bottom evolve from an irregular shape (Figs. 1A,B) to circles (Figs. 1C,D), and their sizes also increase due to a heating-induced rise in contact area between the PSs and the substrate. With a heating time of 40 min the diameter of the pores at the bottom is about 800 nm, near to that of the PSs, and the pores are nearly cylindrical, as shown in Figure 1D. The film thickness and openings at the film surface can be controlled by the electrodeposition time. Samples A,B in Figure 1 were electrodeposited for 15 min. The pore diameters at the film surface are nearly equal to those of the PSs, and almost all the circles at the film surface are in contact with each other. An approximate calculation according to a simple geometrical relationship between the spheres[23] gives film thicknesses of 310 nm and 320 nm, respectively. With a shorter electrodeposition time (8 min), the film thickness is thinner and the pore diameters at the film surface are smaller than those of the PSs, therefore they become separated from each other due to the limitation of the template geometry, as shown in Figure 1C (about 160 nm in thickness). However, if the electrodeposition is long enough, the film thickness will be greater than the distance between the center of the PSs and the substrate, and the pore diameters at the film surface will also be smaller than those of the PSs, as illustrated in Figure 1E (about 940 nm in thickness). Samples C,E were heated for the same time (16 min) before deposition, but the latter was electrodeposited for longer (30 min). Both show a similar morphology from the top view. However, there should be a tunnel between two adjacent pores in sample E, which is induced by the contact area between two adjacent PSs due to heating before deposition.[13]

Similar results were obtained with monolayer templates composed of much smaller PSs. Figure 1F shows the ordered through-pore array fabricated with a 350 nm PS monolayer with heating and electrodeposition times of 3 and 5 min, respectively. It exhibits the same regularity as those formed from the 1000 nm PS monolayer, except for the pore size.

Interestingly, such an ordered porous film can be transferred integrally from one substrate to another by lifting it off on a water surface and picking it up with another substrate, as shown in Figure 2. These substrates can be flat or curved, and the front and back surfaces of the films can be chosen according to the application requirements. Figures 3A,B show the ordered pore arrays on a mica substrate after transferal. These images correspond to the back surfaces of the deposited films shown in Figures 1B,C, respectively. We can thus see more clearly the morphologies of the openings at the pore bottom for the original through-pore films in Figures 1B,C. The sizes of the bottom openings are about 300 and 400 nm, respectively. Figures 3C,D show the ordered porous film on a type of porcelain tube used as a gas sensor. The film corresponds to that shown in Figure 1B. The inset in Figure 3C is a photograph of the tube covered with the gold film and Figure 3D is an enlargement of the zone indicated in Figure 3C. We can see that the film covers the curved surface and that the microstructure has not changed, except that it looks like a tilt view of Figure 1B due to the curved surface. This is of great importance as it means that we can transfer the film to any substrate, especially to a desired but insulating substrate, like mica or a curved surface, on which the film can not be electrodeposited directly, thus overcoming the restriction of electrodeposition to a conducting substrate.

Further experiments showed that the transferability is related to the electrodeposition rate (or deposition potential) and additive agents in the electrolyte, although it is mainly determined by the film-growth mechanism, which itself depends on the nature of the electrolyte. Here, the electrolyte contains $HAuCl_4$, Na_2SO_3, $C_{10}H_{14}N_2O_8Na_2{\cdot}2H_2O$ (EDTA) and K_2HPO_4. The $HAuCl_4$ is the source of the initial Au^{III}, some of which immediately forms Au^{I}.[33,34] Na_2SO_3 acts as a complexing agent, EDTA improves the mechanical properties of the final films, and K_2HPO_4 mainly acts as an auxiliary complexing agent and buffering agent. When the ITO glass covered with the PS monolayer is dipped into the electrolyte, HPO_4^{2-} is adsorbed onto the substrate before deposition. However, the substrate has already been structured with PSs.

ADVANCED MATERIALS

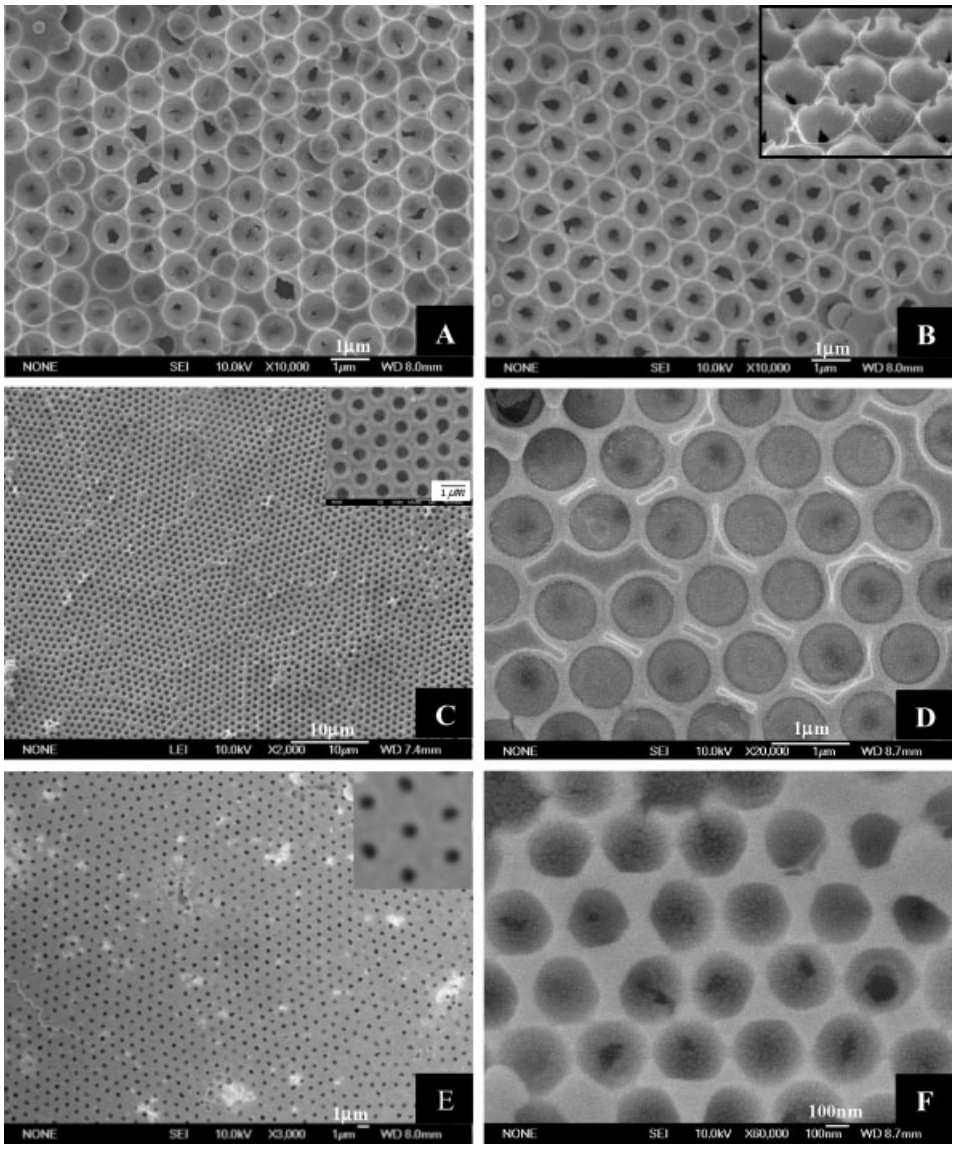

Figure 1. Ordered gold through-pore arrays formed by an electrodeposition method based on a colloidal monolayer. The polystyrene sphere sizes in the monolayer are 1000 nm for (A–E) and 350 nm for (F). All the templates were heated at 110 °C at an electrodeposition potential of 0.7 V vs. SCE. The heating time and the deposition time are, respectively: A) 2 min and 15 min; B) 5 min and 15 min; C) 16 min and 8 min; D) 40 min and 8 min; E) 16 min and 30 min; F) 3 min and 5 min. The insets of (C) and (E) are the corresponding magnified images. The inset of (B) is a tilt view.

The PSs possess some negative charge—the surfaces of the PSs were previously treated with SO_4^{2-}—and this will influence the properties of ITO around the spheres. As a result, the HPO_4^{2-} will be adsorbed onto the substrate away from the spheres, as illustrated in Figure 4A (it is well known that adsorbates on the substrate impede the growth of a film). When the electrodeposition begins the Au crystal nuclei will naturally first be formed in the wedge-shaped regions (or corners) between the PSs and the substrate due to the low energy barrier of nucleation in this area (see Fig. 4B). Since the applied voltage (only 0.7 V vs. SCE) during electrodeposition is not high enough to desorb the adsorbates from the substrate, as the gold grows along the substrate and the PSs from the corners it will also cover the adsorbed area on the substrate. As a result, the thickness of the film at the edge of the pores (at the film surface) will always be thicker than that in the interstitial region between three closely packed spheres, as is clearly illustrated by the tilt view shown in the inset of Figure 1B.

In order to further understand the growth mechanism, we chose to examine an edge region of the sample shown in Figure 1D (Fig. 5). The pores are not ordered, but it is still possible to determine the details of the film growth. In the area without PSs there is no deposited film; the film only grows around PSs. When a single PS is found on the substrate (zone A in Fig. 5), the gold grows around the sphere and forms a hemisphere-like shell of fixed thickness. However,

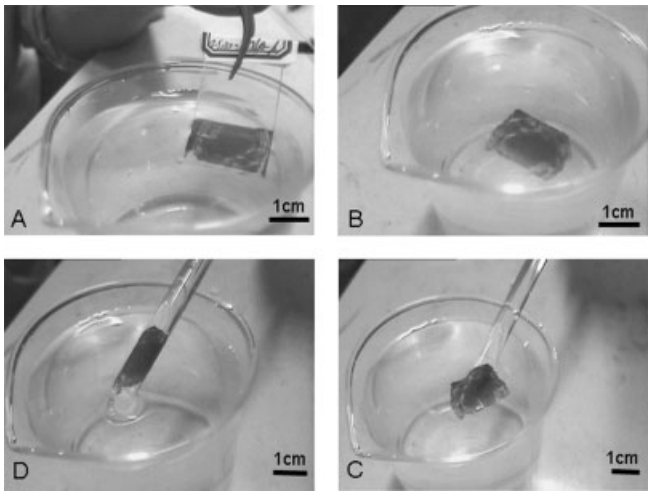

Figure 2. Photographs showing the transfer of the ordered gold porous film on ITO glass to a curved surface (glass rod). A) The ITO glass covered with gold film is dipped into water. B) The gold film is floating on the water. C) The gold film is picked up with a glass rod. D) The gold film is transferred onto the curved surface of the glass rod.

when two spheres are arranged close to each other (zone B), the region between the two spheres and the substrate is obviously different due to the surface charge of the spheres: the amount of adsorbate is less, and as a result, the growth in such regions will be quicker. For the same reason, when three spheres are arranged close to each other (zone C), the growth in the region between the three spheres and the substrate is also quicker than in other regions. A more obvious example is that where the spheres are arranged neither too close nor too far from each other either (zone D). The pores (from the top view) are connected by a film of a certain thickness, and the thickness of the film between the pores is smaller than that surrounding the pores. On this basis, it is easy to understand the formation of the closely packed pore array shown in Figure 1 if all the PSs are closely packed in a monolayer.

The existence of an adsorption layer in some areas between the Au film and the substrate (see Fig. 4A), which weakens the adhesive force between the two, means that the film can be stripped by the surface tension of water. This can be demonstrated more clearly by increasing the electrodeposition rate (or potential). When the potential is increased to 1.7 V vs. SCE, the film does not float off in water. We believe that such a potential is high enough to remove the adsorbates quickly during the initial deposition, therefore the gold film has a much stronger adhesive force with the substrate,[35] and hence cannot be stripped. For the same reason, if we do not add K_2HPO_4 to the electrolyte the film cannot be stripped at any potential, as there is no adsorption on the substrate. This situation has also been found for the electrodeposition of copper.

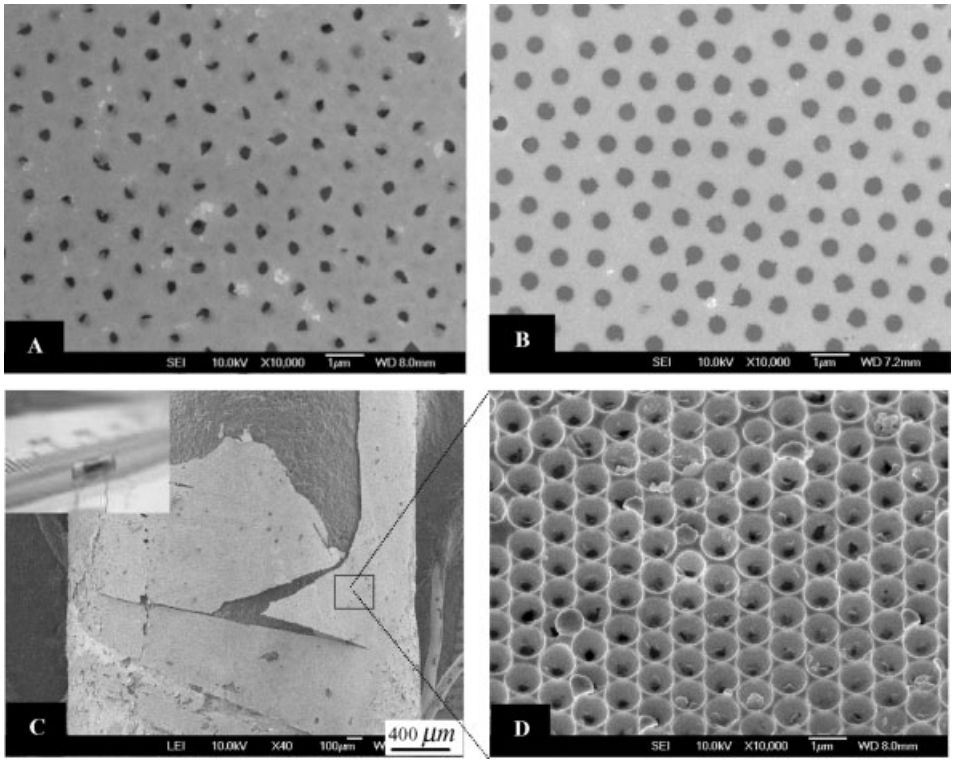

Figure 3. Ordered gold porous films on a mica substrate and on the curved surface of a porcelain tube by lifting off the films from ITO glass. A) The back surface of the film shown in Figure 1B, on mica. B) The back surface of the film shown in Figure 1C, on mica. C) A low-power FE-SEM image of the gold film shown in Figure 1B, on the curved surface of a porcelain tube; the inset is a photo of the tube covered with gold film. D) A magnified image of the zone shown in (C).

ADVANCED MATERIALS

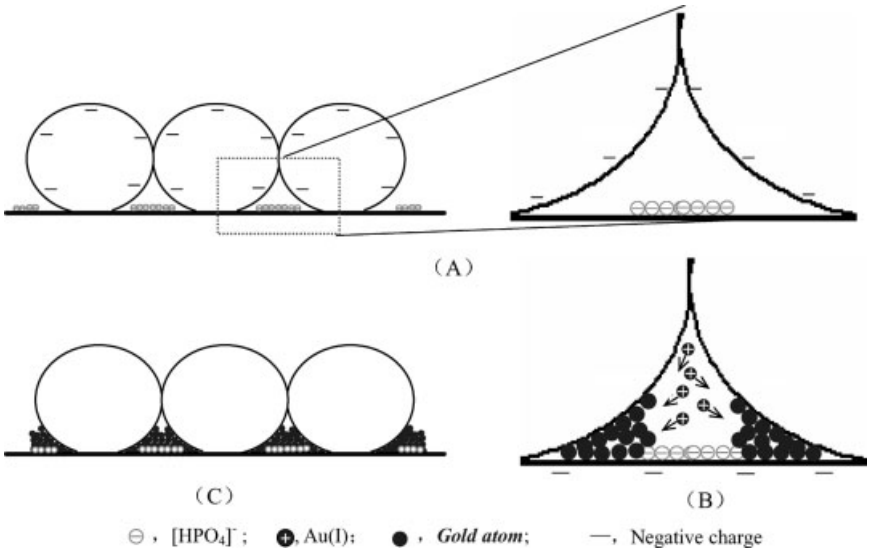

Figure 4. Schematic illustrations of the formation process of ordered gold porous films. A) Monolayer-coated ITO glass in the electrolyte before electrodeposition. B) During initial electrodeposition. C) After electrodeposition.

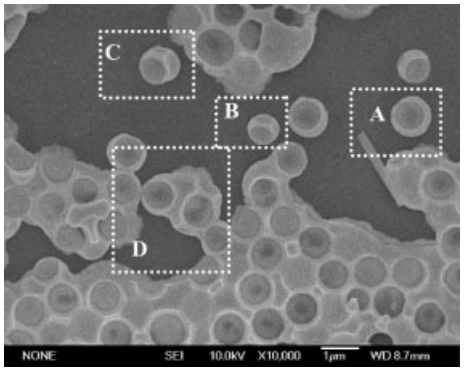

Figure 5. Morphology in the edge region of the sample shown in Figure 1D. A) The pore from one sphere. B) Pores from two spheres in close contact. C) Pores from three spheres in close contact. D) Pores from spheres not in very close contact.

If the electrodeposition onto the monolayer-coated substrate is performed in two different electrolyte solutions separately a bimetal (or bilayer) ordered porous film can be synthesized. We have obtained a Au/Cu bilayer porous film in this manner (not shown here). Further experiments demonstrated that the strategy of electrodeposition based on a colloidal-monolayer template is universal and can be used for the synthesis of other ordered through-pore arrays, including metals, semiconductors, and metal oxides on any conducting substrate, or on an insulating substrate with a flat or curved surface by lifting off and transferring. Using this strategy, we have synthesized a series of ordered through-pore films, such as Cu, Zn, Ag, Ni, ZnO, Eu_2O_3, and Fe_2O_3.

In conclusion, we have presented an electrodeposition approach based on a colloidal-monolayer template, and have synthesized a series of large-area, ordered, through-pore films. The morphology of the films can be controlled simply by heating the colloidal monolayer before deposition and by changing the electrodeposition time. This method is universal and is suitable for other metal and semiconductor ordered through-pore arrays, as well as for the fabrication of bimetal porous films, which might be suitable for the design of new nanodevices. More importantly, the deposited films can be integrally transferred onto any desired insulating substrate, even one with a curved surface, by lifting off, which avoids the restriction of electrodeposition to conducting substrates, and makes it very simple to fabricate such ordered through-pore arrays on any desired substrate by electrodeposition. Experiments reveal that the film transferability could be due to molecule adsorption on the substrate before electrodeposition.

Experimental

The polystyrene sphere suspensions (monodispersed latex spheres stabilized with a slight anionic charge from surface sulfate groups) were bought from Alfa Aesar Corporation. Glass substrates were cleaned according to Dyune's procedure [17]. Large-area ordered colloidal monolayers (more than 1 cm^2) were synthesized on the glass substrates by spin-coating methods on a custom-built spin-coater. ITO-glass substrates were cleaned in acetone, ethanol, and distilled water for 30 min each. The monolayer on the glass substrate was integrally floated off on the distilled water surface, and then picked up with an ITO glass, as illustrated previously [18], followed by heating at 110 °C for a certain time. An aluminum frame and insulating tape were used to cover the edges of the monolayer, as illustrated in Scheme 1D. A solution composed of $HAuCl_4$ (12 $g\,L^{-1}$), EDTA (5 $g\,L^{-1}$), Na_2SO_3 (160 $g\,L^{-1}$), and K_2HPO_4 (30 $g\,L^{-1}$) was used as the electrolyte; the pH value was 5. A graphite plate and a saturated calomel electrode (SCE) were used as the auxiliary and reference electrode, respectively. The distance between the working electrode and the auxiliary electrode was about 4 cm. The electrodeposition was carried out at 45 °C and 0.7 V vs. SCE. After deposition, the monolayer was removed by dissolving in CH_2Cl_2. The morphologies of all the samples were examined on a JSM-6700 field-emission scanning electronic microscope (FE-SEM).

Received: January 5, 2004
Final version: March 29, 2004

[1] S. I. Matsushita, T. Miwa, D. A. Tryk, A. Fujishima, *Langmuir* **1998**, *14*, 6441.
[2] A. Birner, U. Gruning, S. Ottow, A. Schneider, F. Müller, V. Lehmann, H. Föll, U. Gösele, *Phys. Status Solidi A* **1998**, *165*, 111.
[3] M. Imada, S. Noda, A. Chutinan, T. Tokuda, M. Murata, G. Sasaki, *Appl. Phys. Lett.* **1999**, *75*, 316.
[4] N. G. R. Broderick, G. W. Ross, H. L. Offerhaus, D. J. Richardson, D. C. Hanna, *Phys. Rev. Lett.* **2000**, *84*, 4345.
[5] P. M. Tessier, O. D. Velev, A. T. Kalambur, A. M. Lenhoff, J. F. Rabolt, E. W. Kaler, *Adv. Mater*. **2001**, *13*, 396.

[6] T. Tatsuma, A. Ikezawa, Y. Ohko, T. Miwa, T. Matsue, A. Fujishima, *Adv. Mater.* **2000**, *12*, 643.
[7] T. W. Ebbesen, H. J. Lezec, H. F. Ghaemi, *Nature* **1998**, *391*, 667.
[8] Y. Xia, J. Rogers, K. E. Paul, G. M. Whitesides, *Chem. Rev.* **1999**, *99*, 1823.
[9] V. Lehmann, H. Holl, *J. Electrochem. Soc.* **1990**, *137*, 653.
[10] M. H. Stenzel-Rosenbaum, T. P. Davis, A. G. Fane, V. Chen, *Angew. Chem. Int. Ed.* **2001**, *40*, 3428.
[11] P. S. Shah, M. B. Sigman, Jr., C. A. Stowell, K. T. Lim, K. P. Johnston, B. A. Korgel, *Adv. Mater.* **2003**, *15*, 971.
[12] M. Haupt, S. Miller, R. Glass, M. Arnold, R. Sauer, K. Thonke, M. Möller, J. P. Spatz, *Adv. Mater.* **2003**, *15*, 829.
[13] P. Jiang, J. F. Bertone, V. L. Colvin, *Science* **2001**, *291*, 453.
[14] X. Chen, Z. Chen, N. Fu, G. Lu, B. Yang, *Adv. Mater.* **2003**, *15*, 1413.
[15] U. C. Fischer, H. P. Zingsheim, *J. Vac. Sci. Technol. B* **1981**, *19*, 881.
[16] F. Burmeister, C. Schafle, B. Keilhofer, C. Bechinger, J. Boneberg, P. Leiderer, *Adv. Mater.* **1998**, *10*, 495.
[17] C. L. Haynes, R. P. Van Duyne, *J. Phys. Chem. B* **2001**, *105*, 5599.
[18] F. Q. Sun, W. P. Cai, Y. Li, B. Q. Cao, Y. Lei, L. D. Zhang, *Adv. Funct. Mater.* **2004**, *14*, 283.
[19] D. K. Yi, D. Y. Kim, *Nano Lett*. **2003**, *3*, 207.
[20] P. V. Braun, P. Wiltzius, *Nature* **1999**, *402*, 603.
[21] J. E. G. J. Wijnhoven, S. J. M. Zevenhuizen, M. A. Hendriks, D. Vanmaekelbergh, J. J. Kelly, W. L. Vos, *Adv. Mater.* **2000**, *12*, 888.
[22] P. V. Braun, P. Wiltzius, *Adv. Mater*. **2001**, *13*, 482.
[23] P. N. Bartlett, J. J. Baumberg, S. Coyleb, M. E. Abdelsalam, *Faraday Discuss. Chem. Soc.* **2004**, *125*, 117.
[24] G. C. Bond, *Catal. Today* **2002**, *72*, 5.
[25] Z. Ma, S. F. Sui, *Angew. Chem. Int. Ed.* **2002**, *41*, 2176.
[26] W. T. Wallace, R. L. Whetten, *J. Am. Chem. Soc.* **2002**, *124*, 7499.
[27] O. D. Velev, P. M. Tessier, A. M. Lenhoff, E.W. Kaler, *Nature* **1999**, *401*, 548.
[28] Note: A basic essential of this strategy is that the colloid monolayer should cover a conducting surface. However, such a surface is not suitable for synthesizing colloid monolayers in general, and it cannot be washed according to a strict procedure [17] (otherwise the conducting layer may be destroyed). Here we adopt an indirect step to make the colloid monolayer cover the conducting surface.
[29] Y. Yin, Y. Lu, Y. Xia, *J. Am. Chem. Soc.* **2001**, *123*, 771.
[30] D. K. Yi, D. Y. Kim, *Chem. Commun.* **2003**, 982.
[31] J. Aizpurua, P. Hanarp, D. S. Sutherland, M. Käll, G. W. Bryant, F. J. G. de Abajo, *Phys. Rev. Lett.* **2003**, *90*, 057 401.
[32] F. Burmeister, C. Schafle, T. Matthes, M. Böhmisch, J. Boneberg, P. Leiderer, *Langmuir* **1997**, *13*, 2983.
[33] A. He, B. Djurfors, S. Akhlaghi, D. G. Ivey, *Plat. Surf. Finish.* **2002**, *89*, 48.
[34] W. Sun, D. G. Ivey, *Mater. Sci. Eng. B* **1999**, *65*, 111.
[35] R. Winand, *Electrochim. Acta* **1994**, *39*, 1091.

Nanoparticle-Assisted Growth of Porous Germanium Thin Films**

By *Jiann Shieh*,* *Hsuen Li Chen*, *Tsung Shine Ko*, *Hsu Chun Cheng*, and *Tieh Chi Chu*

Since the discovery of its room-temperature luminescence in 1990,[1] much attention has been focused on porous silicon, which is prepared typically by electrochemical anodization in a dilute hydrofluoric acid solution. This fluorescence behavior is of interest because bulk silicon is an indirect bandgap semiconductor, in which crystal momentum is needed to excite an electron from the valence band to the conduction band. Quantum confinement effects of the nanowire skeleton and the state of the surface at the nanocrystal–oxide interface have been suggested to account for the visible luminescence of porous silicon.[2] Relative to silicon, the exciton in germanium has a larger effective Bohr radius, which causes quantum size effects to be more easily achieved.[3] Only a few studies, however, have been carried out on porous germanium because of the lack of adequate procedures for its preparation.[4]

Porous silicon is made up of a network of silicon nanowires. Nanowires can be grown by the vapor–liquid–solid (VLS) growth mechanism, which was first demonstrated by Wagner and Ellis,[5] in which metal catalysts act as energetically favorable sites for the nanowires' growth. The catalyst particles rise up as the nanowire material precipitates from them. This method has been adopted recently to fabricate germanium nanowires by using gold nanoparticles as the seeds.[6–8] Because of the structural instability that results from their high surface energy, an oxide sheath is always found to saturate the dangling bonds on the surface of the sp^3-bonded covalent nanowires.[6,9,10] It has been found that when the silicon nanowires are annealed in hydrogen gas (in order to remove the oxide sheath) the bare nanowires tend to agglomerate.[11] Herein, we report a procedure for growing porous germanium thin films by high-density, inductively coupled plasma chemical vapor deposition (ICPCVD). Compared to other processes (see Table S1 in the Supporting Information),[6–8,12] ICPCVD operates at a lower working pressure (10^{-2} torr),

[*] Dr. J. Shieh, Dr. H. L. Chen,[+] H. C. Cheng
National Nano Device Laboratories
1001-1 Ta-Hsueh Road, 300
Hsinchu (Taiwan ROC)
E-mail: jshieh@ndl.gov.tw
T. S. Ko, Prof. T. C. Chu
Department of Atomic Science
National Tsing Hua University
Hsinchu (Taiwan ROC)
[+] Present address: Department of Materials Science and Engineering, National Taiwan University, Taipei, Taiwan, ROC.

[**] This work was supported by the National Science Council in Taiwan. We thank C. C. Hsu and C. H. Yang for TEM and AES analyses, respectively. We also thank Dr. J. M. Shieh and Dr. B. T. Dai for their help with the ICPCVD system. Supporting Information is available online from Wiley Interscience or from the authors.

 DOI: 10.1002/adma.200306541